

Article

Mechanical Behaviour of Human and Porcine Urethra: Experimental Results, Numerical Simulation and Qualitative Analysis

António Diogo André ^{1,2} , Bruno Areias ¹ , Ana Margarida Teixeira ^{1,2} , Sérgio Pinto ³ and Pedro Martins ^{2,4,*} ¹ Faculty of Engineering, University of Porto, 4200-465 Porto, Portugal² Associated Laboratory of Energy, Transports and Aeronautics (LAETA), Institute of Science and Innovation in Mechanical and Industrial Engineering (INEGI), Faculty of Engineering, University of Porto, 4200-465 Porto, Portugal³ DTx—Laboratório Colaborativo em Transformação Digital, 4800-058 Guimarães, Portugal⁴ Aragonese Foundation for Research and Development (ARAID), Aragón Institute of Engineering Research(i3A), University of Zaragoza, 50015 Zaragoza, Spain

* Correspondence: pedro.sousamartins@gmail.com

Highlights:

- The porcine urethra is a suitable replacement candidate for the human urethra.
- The circumferential urethra should be the object of further investigations.
- The urethra under large deformations may be modelled using FEM and hyperelastic models.

Abstract: Low urinary tract dysfunctions and symptoms (LUTS) affect both men and woman, with the incidence increasing with age. Among the LUTS, urinary incontinence (UI) is a common dysfunction, characterised by the involuntary loss of urine. These medical conditions become debilitating, with a severe impact on patients' routines and overall well-being. To mitigate LUTS-associated symptoms, the mechanical behaviour of both normal and LUTS-affected urethrae can be an important tool. The current work approaches the porcine urethra as a mechanical replacement candidate for the human urethra. It aims to provide a framework based on *in silico* (numerical) simulations and experimental data, to compare the candidate's mechanical behaviour against the human urethra. Porcine urethral samples were mechanically evaluated through low-cycle fatigue tests in both circumferential and longitudinal orientations. The specimens were collected from porcine urethrae from crossbred pigs raised for human consumption. The experimental results were compared with human references found in the literature, with similar experimental conditions. The experimental data were used as the input for the mechanical properties estimation (nonlinear fitting to hyperelastic constitutive models) and for the simulation of the urethral tensile behaviour, using those models. In the longitudinal orientation, the results for the porcine and human urethra were in good agreement, while in the circumferential direction, the differences increased with deformation. Previous data on the mechanical behaviour of the equine urethra is in line with these findings. The nonlinear mechanical behaviour of a porcine urethra was modelled using the finite element method (FEM) and hyperelastic constitutive models. For the longitudinal urethra, the simulation results approximate experimental data for stretches up to $\lambda \approx 1.5$ (50% deformations), whereas for the circumferential urethra, the same was true for stretches up to $\lambda \approx 1.35$ (35% deformations). The hyperelastic models with a higher number of parameters performed better with the third-order Ogden model (six parameters), displaying the best performance among the studied models. The pig urethra is a suitable candidate for an implant targeted at human urethra replacement or as a model to study the human urinary system. Nevertheless, the data available on the circumferential mechanical behaviour need to be consolidated with additional mechanical tests. The tensile behaviour of the porcine urethra over large deformations can be modelled using the third-order Ogden model; however, to extend the modelling capabilities to larger deformations requires the use of hyperelastic models more adequate to soft tissue behaviour.



Citation: André, A.D.; Areias, B.; Teixeira, A.M.; Pinto, S.; Martins, P. Mechanical Behaviour of Human and Porcine Urethra: Experimental Results, Numerical Simulation and Qualitative Analysis. *Appl. Sci.* **2022**, *12*, 10842. <https://doi.org/10.3390/app122110842>

Academic Editors: Ricardo J. Alves de Sousa and Monika Ratajczak

Received: 5 September 2022

Accepted: 19 October 2022

Published: 26 October 2022

Publisher's Note: MDPI stays neutral with regard to jurisdictional claims in published maps and institutional affiliations.



Copyright: © 2022 by the authors. Licensee MDPI, Basel, Switzerland. This article is an open access article distributed under the terms and conditions of the Creative Commons Attribution (CC BY) license (<https://creativecommons.org/licenses/by/4.0/>).

Keywords: porcine urethra; mechanical behaviour; low-cycle fatigue; tensile test; finite element method

1. Introduction

Low urinary tract dysfunctions and symptoms (LUTS) are common conditions for both men and women, with the incidence increasing with age [1,2]. The presence of moderate-to-severe LUTS is estimated worldwide to be 26% for people in their 40s, 33% in their 60s, 42% in their 70s and nearly 50% for those over 80 [3]. These numbers mean that LUTS become a societal problem in ageing demographics, associated to developed countries.

Among the LUTS, urinary incontinence (UI) is a dysfunction which affects nearly 400 million people around the world [4]. Overall, 3 to 11% of the patients are men [5,6]. A UI is defined as an involuntary loss of urine [7,8] and stands out as a widespread LUTS social and hygienic problem. A UI could present as stress, urge, overflow and functional incontinence [9]. Stress urinary incontinence (SUI) is the involuntary loss of urine during daily activities, such as physical activities, laughing or coughing, as a consequence of the increased pressure applied on the abdomen [10]. SUI might be caused by the loss of the anatomic support of the urethra and bladder due to age or a urethral sphincter deficiency [10].

Urge incontinence is characterised by a sudden and strong desire to void, which could be associated to hypersensitivity [10], while overflow incontinence is characterised by urine loss associated with overdistension of the bladder. Finally, functional incontinence occurs due to external factors to the lower urinary tract, such as cognitive or physical limitations that impair the ability to perceive the need to void or to reach a toilet in a timely manner [10].

In addition, these medical conditions may occur alone and combined with other disorders [10]. Whether as a consequence of previous pathologies or combined with them, LUTS add to the suffering of affected patients [10]. A kidney stone is a typical example of a painful urological disorder characterised by crystal concretions within the kidneys, which affects about 12% of the world's population [11,12] and has associated LUTS.

Benign prostatic hyperplasia (BPH), which is another common pathology [13], is defined as an enlargement of the prostate gland and affects up to 60% of men at the age of 90 years old [2]. BPH disease primarily results in a constriction of the urethra and consequently resistance to urinary flow. It could take the form of urgency, frequency, nocturia and a weak urine stream with incomplete emptying [14]. However, if these symptoms are not treated, they could evolve into something more serious, such as urinary retention, recurrent urinary tract infections and/or obstructed uropathy [15].

In general, LUTS-associated pathologies are debilitating conditions with a severe impact on patients' routines and overall well-being [7,8]. There is a notable reduction in social relationships and activities and an impact on self-esteem [16]. Additionally, these disorders lead to expensive health expenditures [14], e.g., in the United States of America, the costs might ascend to 4 billion USD each year [17].

Medical treatments for LUTS have evolved over the last decade, including the availability of numerous drugs, such as α -blockers, 5α -reductase inhibitors, antimuscarinics, phosphodiesterase type 5 inhibitors (PDE5Is) and intradetrusor injections of botulinum toxin [18]. Today, these therapeutics are considered standard procedures [18]; however, not all patients with LUTS respond satisfactorily. In extreme cases, an invasive approach through implantable devices might be the only solution [19], resulting in a significant discomfort among patients.

To mitigate LUTS-associated symptoms and their consequences, the mechanical behaviour of both normal and LUTS-affected urethrae can be an important tool. Because it is difficult to obtain human samples for *ex vivo* experiments [20], a possible research avenue could rely on using a replacement of the human urethra with similar mechanical properties, such as equine, rabbit or porcine urethrae.

Natali et al. [4] carried out a mechanical protocol to characterise horse urethral tissues and structures, including distal and proximal regions and circumferential and longitudinal directions. They performed tensile and stress–relaxation tests to investigate the response of the tissues and inflation tests to study the behaviour of urethral structures. With the elastic and viscous parameters obtained from this work, Natali et al. [20] investigated the mechanical interaction of urethra tissues under occlusion with a prosthesis. They developed a computational model and assumed that equine and human urethra are similar. They were able to characterise the nonlinear mechanical behaviour, using an hyperelastic formulation, and proposed preliminary constitutive parameters. From the same group, Natali et al. [21] also studied the mechanical behaviour of the lower urinary tract, performing inflation tests on segments of horse penile urethrae. From the experimental results, a computational model was developed to interpret the response in pressure–volume–time of the structures. They obtained an elastic modulus of 0.677 ± 0.026 and 0.262 ± 0.006 kPa for the proximal and distal regions, respectively. Concerning the viscous component, the results were $\tau_1 = 0.153 \pm 0.018$ s, $\tau_2 = 17.458 \pm 1.644$ s and $\tau_1 = 0.201 \pm 0.085$, $\tau_2 = 8.514 \pm 1.379$ s for the proximal and distal regions, respectively.

Using and comparing with rabbit urethrae, Wang et al. [22] and Feng et al. [23] studied the mechanical properties and biocompatibilities of several biomaterials, such as polyglycolic acid, to be used as scaffolds. Their final goal was to consider them for urethral regeneration and reconstruction, respectively.

Focusing on porcine tissues, Cunnane et al. [24] evaluated the effects of cryopreservation on the mechanical properties of porcine urethra samples. They performed uniaxial tension and inflation tests and measured the elastic modulus and ultimate tensile strength. In addition, Cunnane et al. [25] characterised human urethral tissue in terms of the mechanics, composition and gross structure in order to produce a more biomimetic scaffold. The mechanical characterisation was made using pressure–diameter and uniaxial extension testing. They concluded that the tissue stiffens as intraluminal pressure is applied. Moreover, the response of the tissue, regarding the elastic and viscous components, was independent of the regional or directional variance.

In the current study, the porcine urethra will be investigated as a possible replacement model for the human urethra, mainly concerning the mechanical behaviour.

The mechanical properties of the porcine urethra, obtained through experimental tests in the longitudinal and circumferential directions, will be used as input data for the finite element method (FEM) simulations. Moreover, the hypothesis of using the mechanical properties of the porcine urethra as a proxy for the mechanical characterisation of the human urethra will be critically evaluated.

Following the principles outlined above, the samples of the porcine urethra were collected from crossbreed male animals (85 kg; 6 months old) within a maximum of two hours after slaughtering. The urethral samples were then mechanically characterised under low-cycle fatigue conditions.

The experimental protocol, which comprises the first part of this research, was followed by the numerical simulations. Their outputs (the FEM simulation results) were then compared with the experimental mechanical behaviour observed under fatigue loading conditions. This comparison intends to evaluate how close to reality the numerical (FEM) models are given the experimental protocol conditions.

2. Materials and Methods

The experimental program is based on the methodology outlined by Masri et al. [26]. The approach allows a direct comparison of the mechanical behaviour of the urethra between porcine (current study) and human subjects (Masri et al. as reference), thus supporting the effort of finding alternatives (as research models, for therapies, etc.) to the human urethra.

To achieve the goal of this study, the following workflow was adopted, Figure 1.

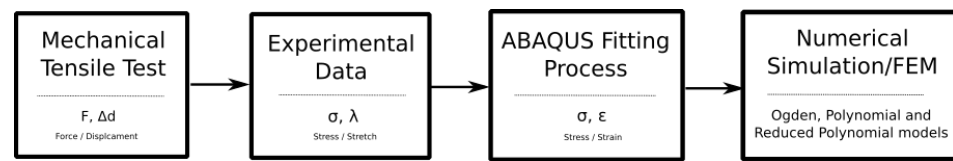


Figure 1. Workflow adopted.

2.1. Methodology Overview

The porcine urethrae were obtained at a slaughterhouse located in Nine-Barcelos, Portugal. The organ collection was carried out under a research agreement between the Portuguese National Authority for Animal Health (DGAV-Direção-Geral de Alimentação e Veterinária) and INEGI (Instituto de Ciência e Inovação em Engenharia Mecânica e Engenharia Industrial), with register number N19128UDER, approved by the ethics committee of DGAV. The agreement guarantees that all sample collection and processing follows Portuguese and European law that guides animal sample collection and processing for research purposes: No. 1 from Article 23 of CE regulation No 1069/2009 of 21 October on health rules as regards animal by-products and derived products not intended for human consumption; Council Directive 93/119/EC of 22 December 1993 on the protection of animals at the time of slaughter or killing; Council Regulation (EC) No. 1099/2009 of 24 September 2009 on the protection of animals at the time of killing.

The samples from porcine urethra were collected from crossbreed male animals (85 kg; 6 months old) within a maximum of two hours after slaughtering.

The organs were kept refrigerated and saturated in saline solution on a thermally insulated box during transportation to the testing site. Then, the mechanical testing was carried out using a prototype tensile testing machine, where the tensile component is equipped with actuators able to exert loads up to 125N and a load cell of 50N was used. The experimental setup is shown in Figure 2.

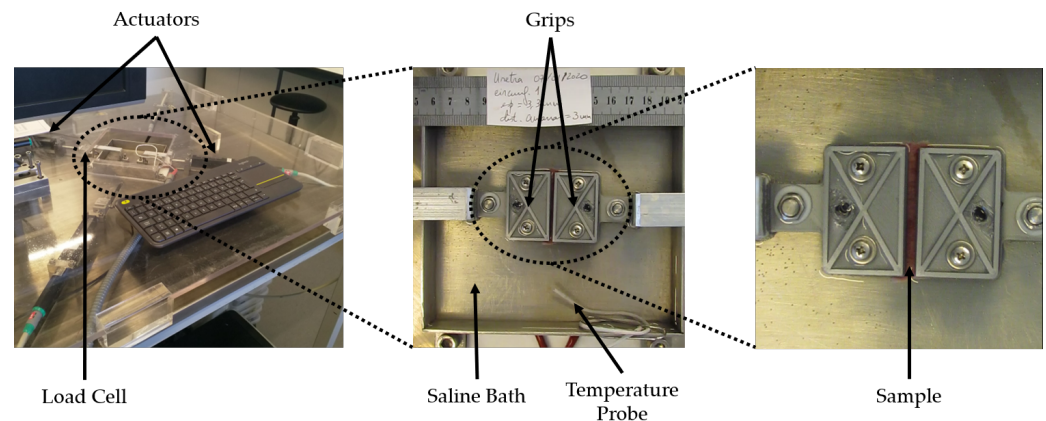


Figure 2. Experimental apparatus used to perform the mechanical tests.

A total of three urethrae from male pigs were used for the mechanical experimental protocol. Following the procedure used by Masri et al. [26], rectangular samples (length: 34.5 mm; width: 10 mm; thickness: ≈ 2.5 mm) were cut from the urethrae specimens along the circumferential and the longitudinal directions. Figure 3 presents a scheme showing the geometric details of the samples and the sample collection sites in relation to the original organ.

During mechanical testing, each sample was put in a saline solution (0.9% sodium chloride) at a temperature of 37 ± 1 °C. They were gripped to the prototype machine (Figure 4) with a distance (l_0) of 2 mm ideally (according to Masri et al. [26]).

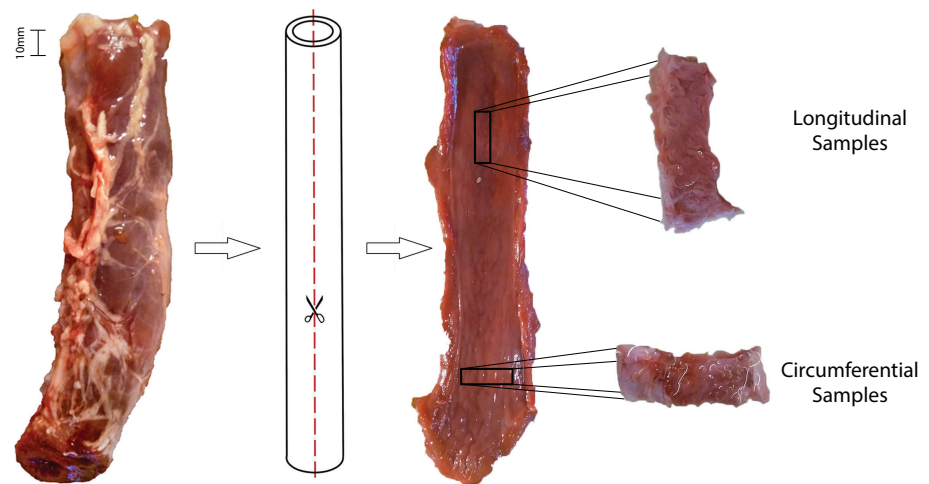


Figure 3. Longitudinal and circumferential urethral samples.

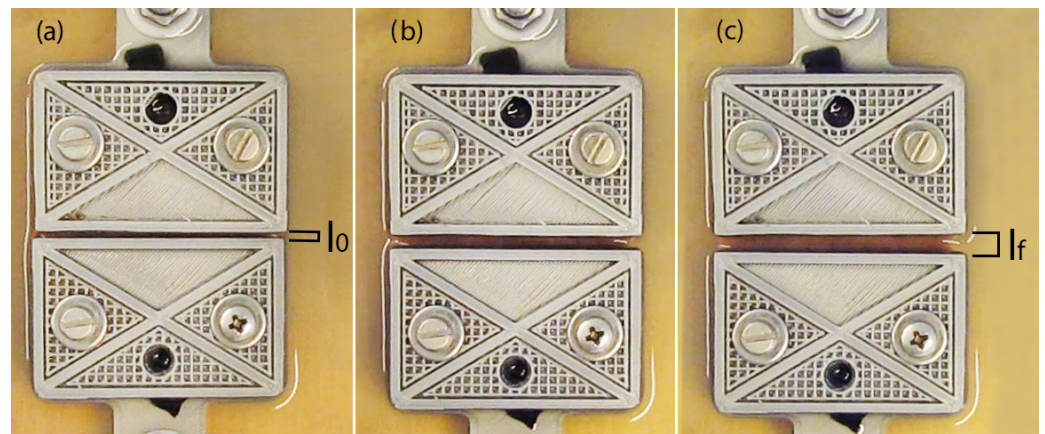


Figure 4. Sample testing for the first cycle: (a) initial deformation at $t = t_0^1 s$; $l = l_0^1 mm$; (b) intermediate deformation; (c) final deformation at $t = t_f^1 s$; $l = l_f^1 mm$.

2.2. Mechanical Tests

The mechanical tests were performed considering the protocol described in Masri et al. [26]. The goal is to have a better understanding of the specimen's mechanical behaviour under low-cycle fatigue tests, thus mimicking physiological conditions of urethral tension, in the longitudinal and circumferential directions.

The fatigue tensile tests were conducted considering a constant velocity of 1 mm/min during the entire procedure. In the successive 7 cycles that comprise the experiment, the maximum stretch increases from the base value ($\lambda = 1$) to 1.1 (1st cycle), 1.2, 1.3, 1.4, 1.5, 1.75 and $\lambda = 2.0$ (7th cycle), being the initial stretch of each cycle (l_0^i) equal to $\lambda = 1$.

A total of 17 samples, obtained from the three urethrae, were tested, corresponding to 8 and 9 samples cut in circumferential and longitudinal orientations, respectively. Figure 4 shows the initial, middle and final moments of a given cycle. During each test, both load (N) and displacement (mm) were continuously recorded at 100 Hz.

2.3. Mathematical Analysis

From the initial 17 samples tested, only 6 samples were included in this study: 3 samples in both circumferential and longitudinal orientations. The exclusion criteria accounted for deviations to the normal experimental protocol, which included slippage and/or misalignment.

For each orientation, the mean and standard deviation were calculated for each cycle. Then, the mean curve obtained was compared with the values presented in literature for human [25,26], porcine [24] and equine [4] urethrae.

Moreover, the mean curve regarding solely the last cycle of the tensile component was used for the FEM simulations and compared with the results of each model considered.

2.4. FEM Simulation

The experimental data of the last tension cycle (7th cycle, $\lambda = 1 \iff 2.0$) were fitted to nonlinear constitutive models using the inbuilt nonlinear fitting capabilities available in ABAQUS software package. The hyperelastic models considered for this approach were Ogden (Equation (1)) [27,28], Polynomial model (Equation (2)) [29,30] and finally Reduced Polynomial (RP) model (Equation (3)) [31].

$$U = \sum_{i=1}^N \frac{2\mu_i}{\alpha_i^2} (\bar{\lambda}_1^{\alpha_i} + \bar{\lambda}_2^{\alpha_i} + \bar{\lambda}_3^{\alpha_i} - 3) + \sum_{i=1}^N \frac{1}{D_i} (J^{el} - 1)^{2i} \tag{1}$$

$$\mu_i, \alpha_i, D_i > 0, i = 1, 2, \dots, N$$

$$U = \sum_{i+j=1}^N C_{i,j} (\bar{I}_1 - 3)^i (\bar{I}_2 - 3)^j + \sum_{i=1}^N \frac{1}{D_i} (J^{el} - 1)^{2i} \tag{2}$$

$$C_{i,j}, D_i > 0, i + j = 1, 2, \dots, N$$

$$U = \sum_{i=1}^N C_{i,0} (\bar{I}_1 - 3)^i + \sum_{i=1}^N \frac{1}{D_i} (J^{el} - 1)^{2i} \tag{3}$$

$$C_{i,0}, D_i > 0, i = 1, 2, \dots, N$$

where U is the strain energy potential, $\bar{\lambda}_1, \bar{\lambda}_2, \bar{\lambda}_3$ are the deviatoric principal stretches, μ_i, α_i, D_i and $C_{i,j}$ are temperature-dependent material parameters, J^{el} is the elastic volume ratio and \bar{I}_1 and \bar{I}_2 are the first and second deviatoric strain invariants [27,29].

The fitting results are an estimation of the parameters associated to each model, i.e., the mechanical properties under a nonlinear framework. They constitute the inputs for the FEM simulations conducted to compare the experimental and numerical results. Several FEM simulations were carried out considering C3D8H elements mesh (8-node hybrid hexahedral element quadratic approach with 8 nodes [29]).

The FEM model was assembled using boundary conditions and imposed displacements similar to the experimental procedure. The model is comprised of 7000 elements and 8946 nodes. A mesh convergence study was performed to make sure that the element size is adequate to achieve an accurate solution (global mesh seed of 0.5 mm). A nonlinear static analysis was conducted. Figure 5 shows the hexahedral element mesh with the imposed displacement and boundary condition.

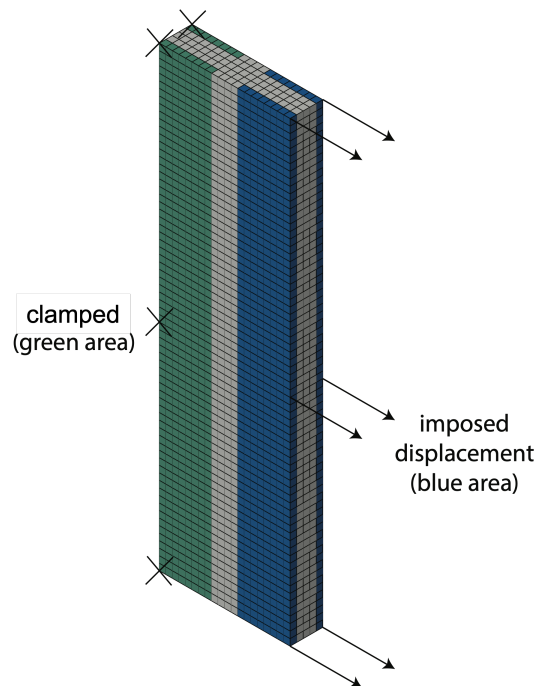


Figure 5. Boundary conditions and displacement imposed to the mesh to conduct FEM simulations. The FEM model mimics the experimental procedure.

3. Results and Discussion

This research aims to investigate the viability of using porcine urethrae as an alternative model to study the mechanical properties and the mechanical behaviour of man's urethra.

3.1. Experimental Results

Figures 6 and 7 present the individual longitudinal and circumferential curves obtained experimentally, along with their respective mean curves.

In Figure 6, the longitudinal curves correspond to the validated mechanical tests (#3). For each cycle of the mean curve, with corresponding stretch values ($\lambda = 1.1, 1.2, 1.3, 1.4, 1.5, 1.75$ and 2.0), the peak stress values are 7, 9, 17, 26, 38, 70 and 106 kPa, respectively.

The circumferential results are shown in Figure 7, where the validated experimental data (#3 samples) and the mean curve are represented. At the peak of each cycle ($\lambda = 1.1, 1.2, 1.3, 1.4, 1.5, 1.75$ and 2.0), the maximum stress is 7, 8, 12, 18, 24, 47 and 74 kPa, respectively.

At each cycle, the longitudinal samples achieved higher peak stress values when compared to the circumferential samples. This could be justified by the orientation of the fibres, which is different for each type of sample. The fibre contribution makes the longitudinal samples stiffer, a phenomena well documented in the literature [26,32,33].

Comparing the current results (porcine urethra) with the human data from Masri et al. (human urethra) [26], we can point out both similarities and differences.

In Figure 8 (longitudinal urethra), the shape similarities between the porcine experimental data (current study) and the results achieved by Masri et al. for the human urethra (using the same experimental protocol) are evident. Still, the results from Masri et al. (full line) are 'softer' than the porcine results (long dashed line). The porcine results' curve (current study) is always above the human results (Masri, [26]) even if the standard deviation (STD) of the pig data (grey ribbon) is taken into consideration. However, these differences are smaller by considering the mean curve of the pig data minus the STD (σ -STD).

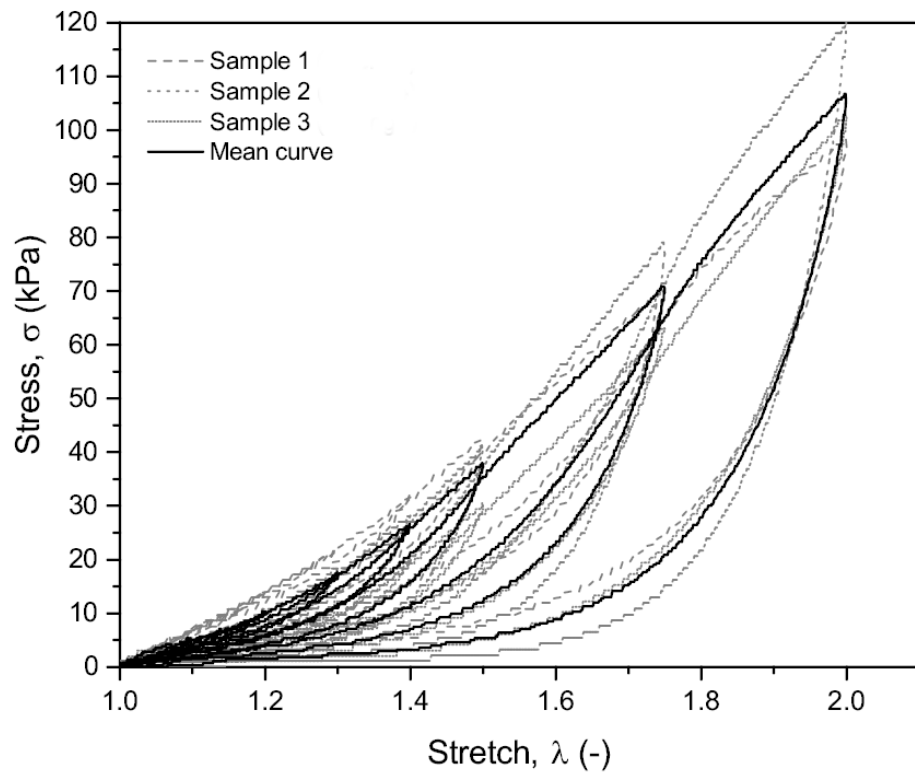


Figure 6. Experimental results and mean curve corresponding to the longitudinal samples from porcine urethra.

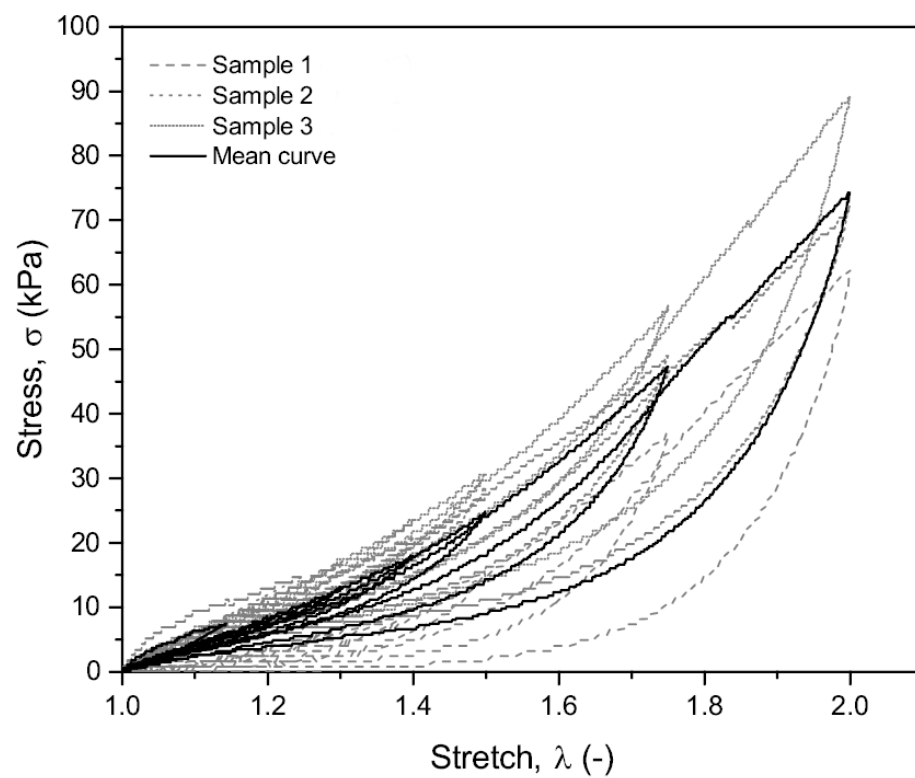


Figure 7. Experimental results and mean curve corresponding to the circumferential samples from porcine urethra.

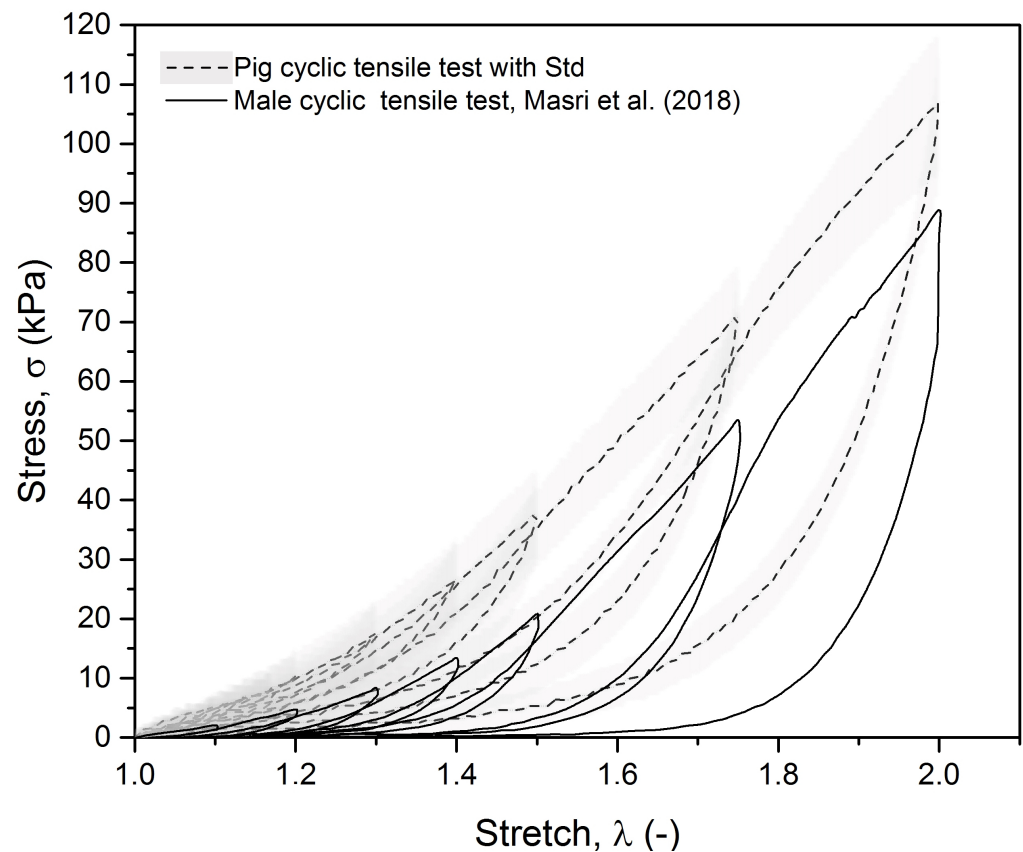


Figure 8. Comparison of the experimental results of longitudinal samples of the urethra from male pig and male human subjects (grey ribbon—STD of the results of the current study).

Recently, Cunnane et al. [25] have studied the mechanical behaviour of the human male urethra, and their results have important differences when compared to those of Masri (human) and the current study (porcine). The longitudinal tensile curves (and the circumferential, which are identical) evidenced much lower stresses for every stretch level considered. The maximum stress achieved, corresponding to the last stretch level considered ($\lambda \approx 2$), was ≈ 6 kPa.

The porcine results (this work) can also be compared with the data from Natali et al. [4] for the horse urethra. For a $\lambda = 1.6$ (60% deformation), these authors obtained a corresponding stress which is approximately half of the porcine results. These differences point to a difference in the stiffness between the tissues (porcine and equine urethrae) in the longitudinal orientation.

A comparison of the experimental data for the circumferential urethrae (porcine—current study vs. human—Cunnane et al. [25]) is presented in Figure 9. The overall mechanical behaviour of both tissues (the curve shape of full and dashed lines) is different. However, several peak maxima (the maximum stress of the load region) have identical intensities if we consider the variability associated with the STD. Considering the tensile test results from Cunnane et al. [25] (human urethra), the specimens tested in a circumferential orientation showed consistently smaller stress levels (≈ 6 kPa for a $\lambda \approx 1.9$) when compared with the porcine results. Comparing the mechanical behaviour in both studies up to their common stretch ($\lambda = 1.6$), they have a modulus in the same order of magnitude, 48 and 39 kPa, respectively.

Recently, Cunnane et al. [24] investigated the mechanical behaviour of the porcine urethra in the circumferential direction. However, these authors reported a stiffer tensile behaviour of the circumferential samples when compared to the results obtained in the current work—for a stretch of $\lambda = 1.6$, the reported Cauchy stress was approximately 250 kPa.

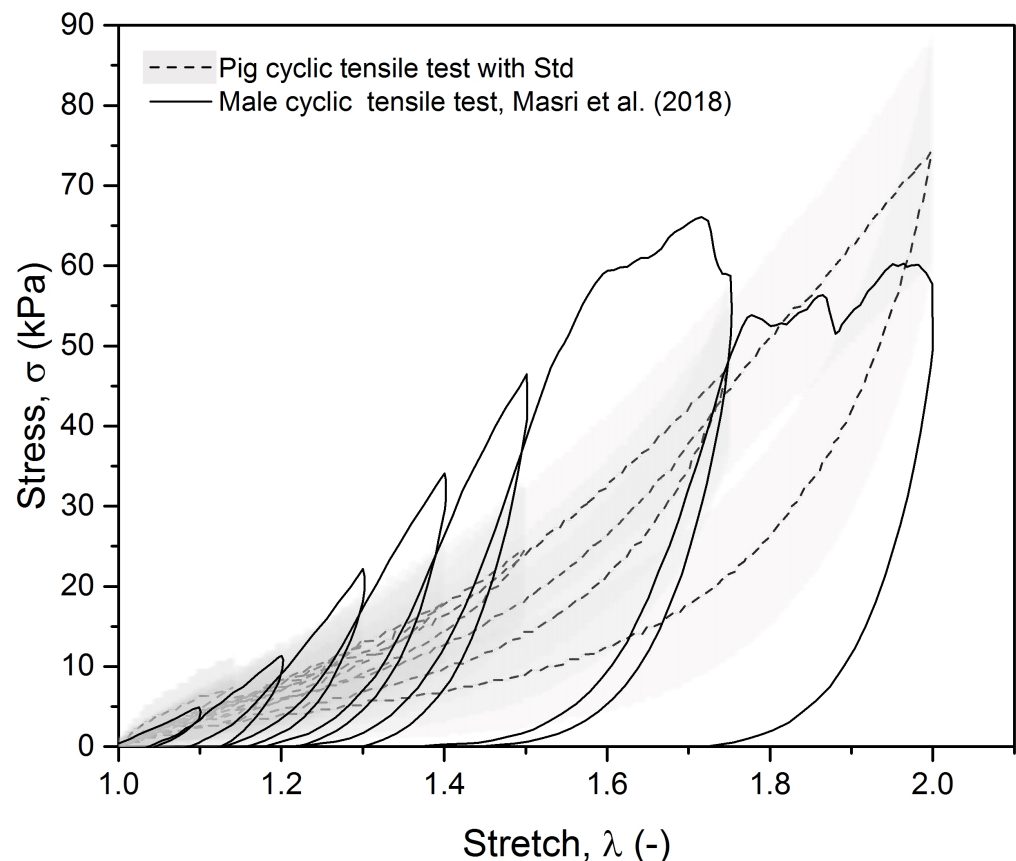


Figure 9. Comparison of the experimental results of circumferential samples of the urethra from male pig and male human subjects (grey ribbon—STD of the results of the current study).

3.2. FEM Simulation

The experimental data presented in Figures 6 and 7, corresponding to the tensile behaviour of the longitudinal and circumferential samples from the porcine urethra, were obtained using the protocol outlined in Section 3.1. The mean value (the point-wise arithmetic mean over the samples considered) of the last cycle (the load–unload cycle corresponding to higher stretch values), together with the FEM model outlined in Figure 5 were the input data for the FEM simulation process. To obtain the material parameters associated to the nonlinear constitutive models corresponding to Equations (1)–(3), the experimental data (in the stress–strain format) were fitted directly by the ABAQUS software package. For the hyperelastic material models available, the software conducts a stability analysis during the fitting process. Those models deemed unsuitable to be used for simulations with the proposed FEM model (due to material instabilities in the experimental strain range) were discarded. Table 1 presents a relation of the viable (stable) models and their material parameters.

Figures 10 and 11 compare the experimental data in the form of point-wise mean curves of longitudinal and circumferential samples, with the corresponding FEM simulations. In general, the same model was stable for both datasets; however, for higher polynomial orders ($n = 5$ and $n = 6$ order), there was a difference—with the fifth-order Reduced Polynomial (RP) model being stable only for the circumferential sample while the sixth-order RP model was stable only for the longitudinal sample.

Considering the longitudinal data (Figure 10), all the models tested could provide an adequate estimation of the experimental data up to a 30% deformation ($\lambda \approx 1.3$). For stretches up to $\lambda \approx 1.5$, there are two clusters of model results. The first cluster includes the third-order Ogden model ($n = 3$) and the $n = 2, 3, 6$ RP models. Despite the significant deviations observed for deformations over 50% ($\lambda > 1.5$), these models seem to follow

the experimental stress evolution. Of the remaining models, the first-order Ogden model ($n = 1$) and specially the Neo-Hookean model, the $n = 1$ RP model displayed the worst performance in modelling the experimental mechanical behaviour of the porcine urethra in the longitudinal direction. In general, the FEM models reached a maximum stress of ≈ 70 kPa while the experimental data reached ≈ 110 kPa, which can be interpreted as the experimental data being 36% stiffer than the simulations for $\lambda = 2.0$ (100% deformation). It is noticeable that the models with a higher number of parameters (Table 1) have a better performance—the third-order Ogden ($k = 6$), sixth-order RP ($k = 6$) and third-order RP ($k = 3$). Conversely, the models with the poorest outcome were those with a lower number of parameters—the first-order Ogden ($k = 2$) and Neo-Hookean model ($k = 1$).

Table 1. Constitutive FEM models considered for this study.

Models	Longitudinal			Circumferential		
Ogden	k	α_k	μ_k	k	α_k	μ_k
$n = 1$	1	7.66217	5.1078×10^{-3}	1	5.46193	9.30213×10^{-3}
$n = 3$	1	2.14665	-4.01108	1	1.22825	-1.27365
	2	2.61517	1.98579	2	2.06915	0.60762
	3	1.64414	2.03311	3	0.25084	0.68139
Reduced Polynomial	k	C_{k0}		k	C_{k0}	
$n = 1$	1	4.78018×10^{-3}		1	7.68995×10^{-3}	
$n = 2$	1	2.35956×10^{-3}		1	5.10340×10^{-3}	
	2	6.85663×10^{-3}		2	3.81972×10^{-3}	
$n = 3$	1	2.88171×10^{-3}		1	5.72309×10^{-3}	
	2	4.17404×10^{-3}		2	1.73464×10^{-3}	
	3	1.56270×10^{-3}		3	9.88421×10^{-4}	
$n = 5$	1	-		1	6.46830×10^{-3}	
	2	-		2	-3.36837×10^{-3}	
	3	-		3	8.66493×10^{-3}	
	4	-		4	-3.84478×10^{-3}	
	5	-		5	5.95269×10^{-4}	
$n = 6$	1	3.31451×10^{-3}		1	-	
	2	8.34169×10^{-4}		2	-	
	3	4.97211×10^{-3}		3	-	
	4	1.60414×10^{-3}		4	-	
	5	-2.09095×10^{-3}		5	-	
	6	4.16037×10^{-4}		6	-	

Regarding the circumferential data (Figure 11), the only reliable model in the $1.0 \leq \lambda \leq 1.2$ range was the third-order Ogden model ($n = 3$). This model could be used to approximate the mechanical behaviour of the circumferential porcine urethra to deformations as high as 35% ($\lambda = 1.35$), despite the evident divergence (between the third-order Ogden and experimental data) for deformations over 30% ($\lambda > 1.3$). None of the remaining constitutive models (Ogden ($n = 1$), Neo-Hookean, RP ($n = 2$), Yeoh and RP ($n = 5$)) were able to approximate the experimental curve across the stretch range considered. On average, the FEM models reached ≈ 25 kPa for 100% deformation ($\lambda = 2.0$), while the experimental data had a maximum stress 3 times higher ≈ 75 kPa. Again, the third-order Ogden model ($n = 3$) had a better performance, despite the clear deviation (max stress of 55 kPa) from the experimental data.

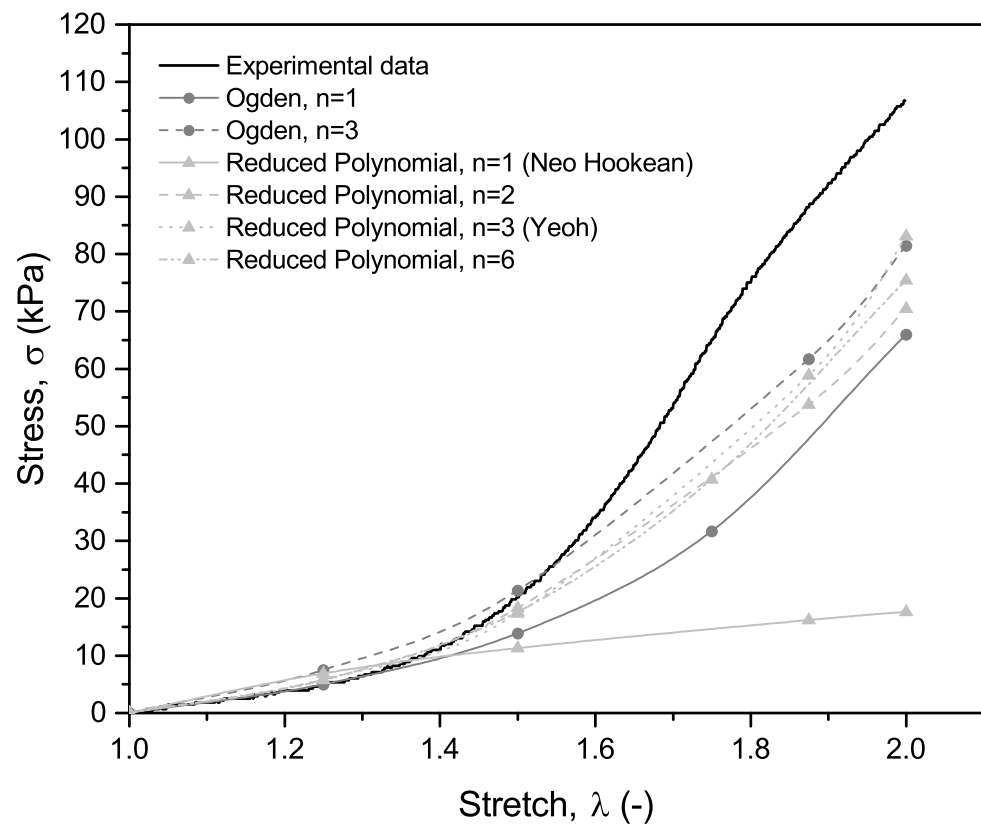


Figure 10. Comparison of longitudinal experimental mean curve (last tensile cycle) and FEM curves.

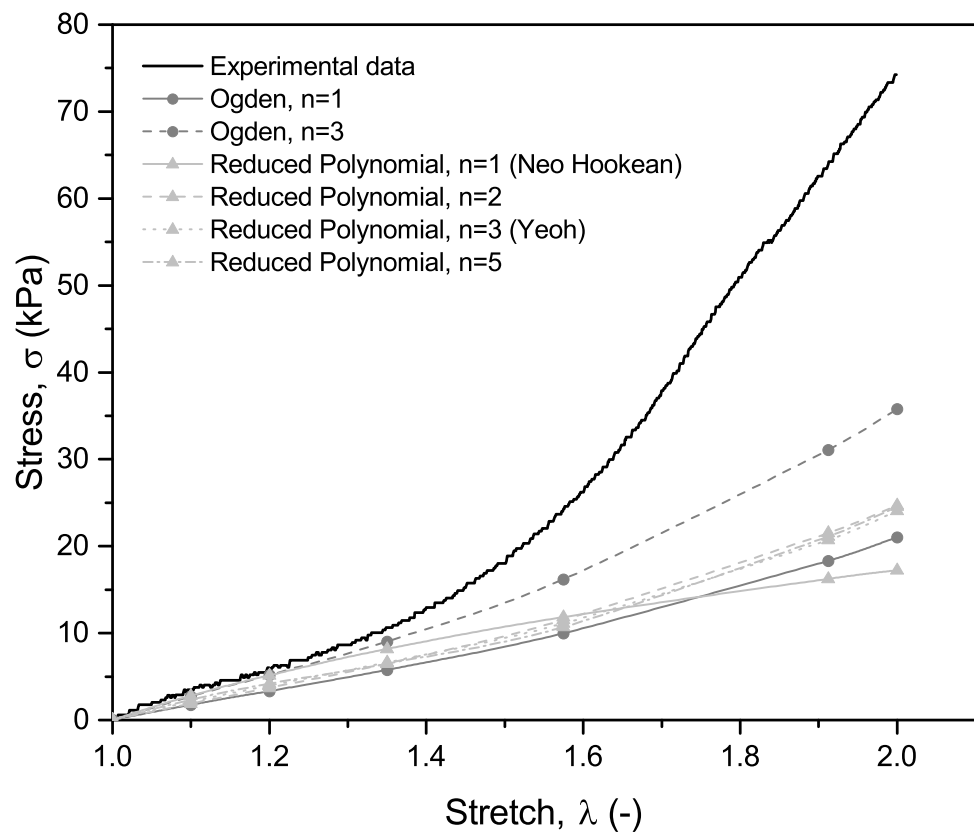


Figure 11. Comparison of circumferential experimental mean curve (last tensile cycle) and FEM curves.

4. Conclusions and Future Perspectives

The current work aims to establish a framework to evaluate the mechanical behaviour of potential substitutes for the human urethra. Those candidates may be either synthetic or biological, provided that biocompatibility is a priori guaranteed (using biocompatible materials) or achievable with tissue processing techniques, such as decellularisation. Our approach includes both the experimental characterisation of the candidates, as well as FEM simulations to model the experimental tensile behaviour of both longitudinal and circumferential urethral samples using FEM. As a first iteration, aimed at being reproducible and easier to implement, we consider hyperelastic constitutive models readily available in the ABAQUS software package. Due to the proximity between pig and human anatomies, there have been many studies using pig tissues and organs as potential candidates for human implantation [34,35]. Therefore, pig urethra was chosen as the potential candidate for human urethra replacement and evaluated using the approach described in the paper.

From the existing literature on urethral mechanics, there are experimental results from different urethral models that can be compared with our experimental results. The works from Natali et al. [4,20,21] on the mechanical properties of the equine urethra are frequently considered a benchmark in the field. These authors have made the most detailed study of a urethral model that can be found in the literature. Our results for the longitudinal porcine urethra were stiffer than the equine data from Natali et al. [4], with the porcine urethra achieving stress values with twice the magnitude. These differences point to microstructural causes (the quantity and spatial arrangement of elastin and collagen) that should be considered in future iterations of this work.

Considering the longitudinal urethra, the porcine data (Cunnane et al. [25] and our data, Figure 8) are in good agreement with the available human data (Masri et al. [26] and Cunnane et al. [24]).

For the circumferential urethra, the pig (our data and Cunnane et al. [25]) and human data [26] (Figure 9) do not display the same level of agreement as the longitudinal results did. In particular, the results from Cunnane et al. [25] for the porcine model are much more stiffer than those found in the literature. Some differences between the human and porcine cyclic tests could be justified, besides the inter-species differences, by the age gap of the male urethras—an average of 84 years old [26] for the human sample and 6 months old for the porcine sample.

Overall, the pig urethra is a good candidate for an implant targeted at human urethra replacement or as a model to study the human urinary system. This is especially true for the longitudinal urethra and deserves further investigation for the circumferential urethra.

The tensile behaviour of porcine urethra was modelled using the hyperelastic constitutive models available in the ABAQUS software package. Both the longitudinal (Figure 10) and circumferential (Figure 11) datasets were considered. The tensile behaviour of the longitudinal urethra was estimated for stretches up to $\lambda \approx 1.5$ (50% deformations), whereas for the circumferential urethra, the same was true for stretches up to $\lambda \approx 1.35$ (35% deformations). In both cases, the models with a higher number of parameters ($k > 3$) performed better than models with a small number of parameters. Overall, the third-order Ogden model ($n = 3, k = 6$) had the best performance, while the Neo-Hookean model ($n = 1, k = 1$) had the worst performance.

Several improvements can be considered for future iterations of the current work. At the experimental protocol and setup levels, the introduction of different mechanical tests to complement and extend the mechanical characterisation is worth careful consideration. Pressure tests, besides uniaxial tests, could be crucial for a better understanding of the mechanical behaviour of the porcine urethra. The experimental approach proposed by Cunnane et al. [25] and the methodology followed by Natali et al. [4,20,21] are fundamental references for future works. These authors include pressure–diameter tests as well as the viscous responses of the tissue to extension, to complement tensile testing. Microstructural characterisation (using histology) is another aspect to take into consideration,

because it opens many possibilities in terms of FEM modelling (improved geometries, tissue differentiation, etc.) and can provide a basis for a urethral model comparison.

At the simulation level, the use of other constitutive models may contribute to improve the simulations over higher stretch ranges. In particular, models such as the Holzapfel–Gasser model [36] may become instrumental to extend the current study. This hyperelastic model was developed to model arteries but has been successfully applied to other biological structures with embedded fibres, such as vaginal tissue. It can also be used with histological data [37,38] for the very accurate modelling of complex (tridimensional) loading conditions.

Despite its simplicity, the approach followed in this paper can be understood as a simple and fast tool to evaluate the mechanical behaviour of potential substitutes for the human urethra.

Author Contributions: Conceptualisation, A.D.A.; experimental methodology, A.D.A., S.P. and A.M.T.; software, A.D.A. and B.A.; validation, P.M.; formal analysis, P.M.; investigation, A.D.A.; resources, A.D.A.; writing—original draft preparation, A.D.A.; writing—review and editing, A.M.T., B.A. and P.M.; visualisation, A.D.A. and P.M.; supervision, P.M.; project administration, P.M.; funding acquisition, P.M. All authors have read and agreed to the published version of the manuscript.

Funding: The authors gratefully acknowledge funding from FCT, Portugal, under grant SFRH/BPD/111846/2015, SFRH/BD/147807/2019 and 2020.08718.BD, and projects UROSPHINX—Project 16842 (COMPETE2020), and MImBI—PTDC/EME-APL/29875/2017, financed through FEDER and FCT. The authors also acknowledge the funding provided by LAETA, under project UIDB/50022/2020.

Institutional Review Board Statement: Ethical review and approval were waived for this study because INEGI and DGAV (Direção-Geral da Alimentação e Veterinária, Portugal) celebrated protocol with registry number N19128UDER. Such protocol authorises INEGI to collect animal tissue in slaughterhouses for research/educational purposes. Moreover, all procedures respected the conditions imposed by Regulation (EC) No. 1069/2009 of 21 October, on health rules concerning animal by-products and derived products not intended for human consumption.

Informed Consent Statement: Not applicable.

Data Availability Statement: The data that support the findings of this study are available from the corresponding author, Pedro Martins, upon reasonable request.

Acknowledgments: *In memoriam:* The authors would like to dedicate this work to the memory of Mário João Gomes. Mário was a medical doctor, a urologist, with a commitment to research that relied on a constant exercise of humanity and kindness. He had a deep care for those who have worked with him, to the extent of asking to read, correct and improve the project that gave birth to this research, in his deathbed. We owe to the MD, the researcher and the man a debt of gratitude. Thank you Mário João! The authors thank and acknowledge the guidance and support of Rui Simeão Versos (MD). His support at the beginning of this research was instrumental for its success. The authors thank Carnes Landeiro—Rua de Landeiro—Silveiros—Barcelos Apartado 11-EC Nine 4776-909 NINE PORTUGAL for the specimens donation.

Conflicts of Interest: The authors state that they have no financial, professional or other personal involvement in any product, service and/or company that would possibly affect their stance.

Abbreviations

The following abbreviations are used in this manuscript:

LUTS	Low urinary tract dysfunctions and symptoms
UI	Urinary incontinence
SUI	Stress urinary incontinence
BPH	Benign prostatic hyperplasia
PDE5Is	Phosphodiesterase type 5 inhibitors
FEM	Finite element method
STD	Standard deviation
DGAV	Direção-Geral da Alimentação e Veterinária
INEGI	Instituto de Ciência e Inovação em Engenharia Mecânica e Engenharia Industrial

References

1. Kim, K.H.; Ahn, B.; Lim, S.K.; Han, W.K.; Kim, J.H.; Rha, K.H.; Kim, J. Indenter Study: Associations between prostate elasticity and lower urinary tract symptoms. *Urology* **2014**, *83*, 544–549. [CrossRef] [PubMed]
2. Lim, K.B. Epidemiology of clinical benign prostatic hyperplasia. *Asian J. Urol.* **2017**, *4*, 148–151. [CrossRef] [PubMed]
3. McVary, K.T. BPH: Epidemiology and comorbidities. *Am. J. Manag. Care* **2006**, *12*, S122–S128. [PubMed]
4. Natali, A.N.; Carniel, E.L.; Frigo, A.; Pavan, P.G.; Todros, S.; Pachera, P.; Fontanella, C.G.; Rubini, A.; Cavicchioli, L.; Avital, Y.; et al. Experimental investigation of the biomechanics of urethral tissues and structures. *Exp. Physiol.* **2016**, *101*, 641–656. [CrossRef]
5. Buckley, B.S.; Lapitan, M.C.M. Prevalence of Urinary Incontinence in Men, Women, and Children—Current Evidence: Findings of the Fourth International Consultation on Incontinence. *Urology* **2010**, *76*, 265–270. [CrossRef]
6. Nitti, V.W. The Prevalence of Urinary Incontinence. *Rev. Urol.* **2001**, *3*, 2–6.
7. Wyndaele, M.; Hashim, H. Pathophysiology of urinary incontinence. *Surgery* **2017**, *6*, 287–292. [CrossRef]
8. Hall, C.D.; Rabin, J.M. Urinary incontinence. *Med. Update Psychiatr.* **1996**, *1*, 71–76. [CrossRef]
9. Fantl, J.A.; Newman, D.; Colling, J. *Urinary Incontinence in Adults: Acute and Chronic Management*; U.S. Department of Health and Human Services: Washington, DC, USA, 1996.
10. Naughton, M.J.; Wyman, J.F. Quality of Life in Geriatric Patients with Lower Urinary Tract Dysfunction. *Am. J. Med. Sci.* **1997**, *314*, 217–227. [CrossRef]
11. Hornberger, B.; Bollner, M.R. Kidney Stones. *Physician Assist. Clin.* **2018**, *3*, 37–54. [CrossRef]
12. Alelign, T.; Petros, B. Kidney Stone Disease: An Update on Current Concepts. *Adv. Urol.* **2018**, *2018*, 3068365. [CrossRef] [PubMed]
13. Idzenga, T.; Pel, J.J.; Mastrigt, R.V. A Biophysical Model of the Male Urethra: Comparing Viscoelastic Properties of Polyvinyl Alcohol Urethras to Male Pig Urethras. *Urol. Nephrol.* **2006**, *25*, 451–460. [CrossRef] [PubMed]
14. Keplen, S.A.; McVary, K.T. *Male Lower Urinary Tract Symptoms and Benign Prostatic Hyperplasia*; Wiley Blackwell: Hoboken, NJ, USA, 2014.
15. Roehrborn, C.G.; McConnell, J.D.; Saltzman, B.; Bergner, D.; Gray, T.; Narayan, P.; Cook, T.J.; Johnson-Levonas, A.O.; Quezada, W.A.; Waldstreicher, J.; et al. Storage (Irritative) and Voiding (Obstructive) Symptoms as Predictors of Benign Prostatic Hyperplasia Progression and Related Outcomes. *Eur. Urol.* **2002**, *42*, 1–6. [CrossRef]
16. Coyne, K.S.; Wein, A.J.; Tubaro, A.; Sexton, C.C.; Thompson, C.L.; Kopp, Z.S.; Aiyer, L.P. The burden of lower urinary tract symptoms: Evaluating the effect of LUTS on health-related quality of life, anxiety and depression: EpiLUTS. *BJU Int.* **2009**, *103*, 4–11. [CrossRef] [PubMed]
17. Taub, D.A.; Wei, J.T. The economics of benign prostatic hyperplasia and lower urinary tract symptoms in the United States. *Curr. Urol. Rep.* **2006**, *7*, 272–281. [CrossRef]
18. Peyronnet, B.; Brucker, B.M.; Michel, M.C. Lower Urinary Tract Symptoms: What’s New in Medical Treatment? *Eur. Urol. Focus* **2018**, *4*, 17–24. [CrossRef]
19. Chong, J.T.; Simma-Chiang, V. A historical perspective and evolution of the treatment of male urinary incontinence. *Neurol. Urodyn.* **2017**, *37*, 1169–1175. [CrossRef]
20. Natali, A.N.; Carniel, E.L.; Fontanella, C.G.; Frigo, A.; Todros, S.; Rubini, A.; De Benedictis, G.M.; Cerruto, M.A.; Artibani, W. Mechanics of the urethral duct: Tissue constitutive formulation and structural modeling for the investigation of lumen occlusion. *Biomech. Model. Mechanobiol.* **2017**, *16*, 439–447. [CrossRef]
21. Natali, A.N.; Carniel, E.L.; Frigo, A.; Fontanella, C.G.; Rubini, A.; Avital, Y.; De Benedictis, G.M. Experimental investigation of the structural behavior of equine urethra. *Comput. Methods Programs Biomed.* **2017**, *141*, 35–41. [CrossRef]
22. Wang, B.; Lv, X.; Li, Z.; Zhang, M.; Yao, J.; Sheng, N.; Lu, M.; Wang, H.; Chen, S. Urethra-inspired biomimetic scaffold: A therapeutic strategy to promote angiogenesis for urethral regeneration in a rabbit model. *Acta Biomater.* **2016**, *16*, 247–258. [CrossRef]
23. Feng, C.; Xu, Y.M.; Fu, Q.; Zhu, W.D.; Cui, L.; Chen, J. Evaluation of the biocompatibility and mechanical properties of naturally derived and synthetic scaffolds for urethral reconstruction. *J. Biomed. Mater. Res.* **2010**, *94*, 317–325. [CrossRef] [PubMed]
24. Cunnane, C.V.; Croghan, S.M.; Walsh, M.T.; Cunnane, E.M.; Davis, N.F.; Flood, H.D.; Mulvihill, J.J. Cryopreservation of porcine urethral tissue: Storage at $-20\text{ }^{\circ}\text{C}$ preserves the mechanical, failure and geometrical properties. *J. Mech. Behav. Biomed. Mater.* **2021**, *119*, 104516. [CrossRef] [PubMed]
25. Cunnane, E.M.; Davis, N.F.; Cunnane, C.V.; Lorentz, K.L.; Ryan, A.J.; Hess, J.; Weinbaum, J.S.; Walsh, M.T.; O’Brien, F.J.; Vorp, D.A. Mechanical, compositional and morphological characterisation of the human male urethra for the development of a biomimetic tissue engineered urethral scaffold. *Biomaterials* **2021**, *269*, 120651. [CrossRef] [PubMed]
26. Masri, C.; Chagnon, G.; Favier, D.; Sartelet, H.; Girard, E. Experimental characterization and constitutive modeling of the biomechanical behavior of male urethra tissues validated by histological observations. *Biomech. Model. Mechanobiol.* **2018**, *17*, 939–950. [CrossRef]
27. ABAQUS Theory Manual. Available online: <https://classes.engineering.wustl.edu/2009/spring/mase5513/abaqus/docs/v6.6/books/stm/default.htm> (accessed on 13 July 2022).
28. Ogden, R.W. *Non-Linear Elastic Deformations*; Dover Publications Inc.: New York, NY, USA, 1997.

29. Dassault Systemes. *ABAQUS Analysis User's Guide*; Available online: <http://130.149.89.49:2080/v2016/books/usb/default.htm> (accessed on 10 June 2022).
30. Esmail, J.F.; Mohamedmeki, M.Z.; Ajeel, A.E. Using the uniaxial tension test to satisfy the hyperelastic material simulation in ABAQUS. *IOP Conf. Ser. Mater. Sci. Eng.* **2020**, *888*, 012065. [[CrossRef](#)]
31. Seibert, D.J.; Schoche, N. Direct Comparison of Some Recent Rubber Elasticity Models. *Rubber Chem.-Technol.-Rubber Rev.* **2000**, *73*, 366–384. [[CrossRef](#)]
32. Müller, B.; Schulz, G.; Herzen, J.; Mushkolaj, S.; Bormann, T.; Beckmann, F.; Püschel, K. Morphology of urethral tissues. In Proceedings of the Developments in X-ray Tomography VII. International Society for Optics and Photonics, San Diego, CA, USA, 20 September 2010; Volume 7804, p. 78040D. [[CrossRef](#)]
33. Lim, S.H.; Wang, T.J.; Tseng, G.F.; Lee, Y.F.; Huang, Y.S.; Chen, J.R.; Cheng, C.L. The distribution of muscles fibers and their types in the female rat urethra: Cytoarchitecture and three-dimensional reconstruction. *Anat. Rec.* **2013**, *296*, 1640–1649. [[CrossRef](#)]
34. Cone, S.G.; Warren, P.B.; Fisher, M.B. Rise of the Pigs: Utilization of the Porcine Model to Study Musculoskeletal Biomechanics and Tissue Engineering During Skeletal Growth. *Tissue Eng. Part Methods* **2017**, *23*, 763–780. [[CrossRef](#)]
35. Ribitsch, I.; Baptista, P.M.; Lange-Consiglio, A.; Melotti, L.; Patruno, M.; Jenner, F.; Schnabl-Feichter, E.; Dutton, L.C.; Connolly, D.J.; van Steenbeek, F.G.; et al. Large Animal Models in Regenerative Medicine and Tissue Engineering: To Do or Not to Do. *Front. Bioeng. Biotechnol.* **2020**, *8*, 972. [[CrossRef](#)]
36. Gasser, T.C.; Ogden, R.W.; Holzapfel, G.A. Hyperelastic modelling of arterial layers with distributed collagen fibre orientations. *J. R. Soc. Interface* **2006**, *3*, 15–35. [[CrossRef](#)]
37. Rynkevic, R.; Ferreira, J.a.; Martins, P.; Parente, M.; Fernandes, A. Linking hyperelastic theoretical models and experimental data of vaginal tissue through histological data. *J. Biomech.* **2019**, *82*, 271–279. [[CrossRef](#)] [[PubMed](#)]
38. Ferreira, J.P.S.; Rynkevic, R.; Martins, P.A.L.S.; Parente, M.P.L.; Famaey, N.M.; Deprest, J.; Fernandes, A.A. Predicting the mechanical response of the vaginal wall in ball burst tests based on histology. *J. Biomed. Mater. Res. Part Appl. Biomater.* **2019**, *108*, 1925–1933. [[CrossRef](#)] [[PubMed](#)]